

Stereoelectronic Contributions to Long-Range ^1H – ^1H Coupling Constants¹

Eduardo M. Sproviero and Gerardo Burton*

Departamento de Química Orgánica, Facultad de Ciencias Exactas y Naturales, Universidad de Buenos Aires, Pabellón 2, Ciudad Universitaria, (C1428EHA) Buenos Aires, Argentina

Received: January 18, 2002; In Final Form: May 7, 2002

The contribution of stereoelectronic interactions to NMR coupling constants $^3J_{\text{HH}}$ and $^4J_{\text{HH}}$ has been examined using ab initio calculations and natural bond orbital (NBO) analysis on four model compounds: ethane, propane, propene, and methylcyclopropane. The main stereoelectronic contributions to the couplings originate in three-bond (vicinal) interactions and in through-space interactions. In ethane, besides the main contribution of the $\sigma(\text{C}-\text{H}) \rightarrow \sigma^*(\text{C}-\text{H})$ interaction, other interactions present in the molecule make a decisive contribution to the angular dependence of 3J . In the $\text{H}_1-\text{C}-\text{C}-\text{C}-\text{H}_{\text{anti}}$ moiety of propane, $^4J_{\text{HH}}$ has important contributions from vicinal interactions that include the anti proton while in the $\text{H}_1-\text{C}-\text{C}-\text{C}-\text{H}_{\text{gauche}}$ moiety the main contributions are vicinal interactions that include H_1 . In alkene fragments, vicinal interactions that involve the π orbitals are the most important contributions to the couplings. Sigma vicinal interactions, which include orbitals corresponding to C–H bonds that involve either of the coupled protons, are crucial to elucidate differences between cisoid and transoid coupling constants. In the case of methylcyclopropane, the most important contributions to the coupling of the syn cyclopropyl H come from the $\sigma(\text{C}-\text{H}) \rightarrow \sigma^*(\text{C}_{\text{cyclopropane}}-\text{C}_{\text{cyclopropane}})$ and $\sigma(\text{C}_{\text{cyclopropane}}-\text{C}_{\text{cyclopropane}}) \rightarrow \sigma^*(\text{C}-\text{H})$ vicinal interactions (where the H corresponds to the non-cyclopropyl hydrogen). The concerted effect of several interactions that contribute toward a trend similar to that shown by allyl–vinyl proton couplings is in accordance with a significant π contribution of the $\text{C}_{\text{cyclopropane}}-\text{C}_{\text{cyclopropane}}$ bond. For the anti cyclopropyl proton, vicinal interactions of the form $\sigma(\text{C}-\text{H}_{\text{anti}}) \rightarrow \sigma^*(\text{C}_{\text{cyclopropane}}-\text{C})$ and $\sigma(\text{C}_{\text{cyclopropane}}-\text{C}) \rightarrow \sigma^*(\text{C}-\text{H}_{\text{anti}})$ are the main contributors to the angular variation of the couplings, similar to what happens to the anti proton in propane. As a whole, the overall behavior of these couplings resembles that of the equivalent proton in propane. In addition, in this case there is not a unique set of interactions which accounts for the overall angular variation of 4J .

1. Introduction

Very early in the history of NMR spectroscopy interproton couplings were recognized as powerful tools for elucidating molecular structure.² Since the pioneering work of Ramsey,³ it has been considered that these couplings are dominated by the Fermi contact term. Thus, couplings through a saturated pathway are characterized by a high stereospecificity, and for certain configurations of the σ -type pathway connecting the coupled nuclei, they attenuate rapidly with the number of bonds.⁴ For couplings between nuclei connected by an unsaturated pathway, the spin polarization of the π electronic system by a σ – π exchange mechanism was recognized, since the Fermi contact interaction cannot initiate in a π -type orbital.⁵ One of the main features of the π -transmitted component is its sign, which alternates with the number of bonds separating the coupled protons⁷ (n): $\text{Sg}\{^nJ^\pi\} = (-1)^{n+1}$. In benzylic couplings, Hoffman⁶ identified hyperconjugative interactions as the mechanism that originates the spin polarization of the aromatic π system. Early reviews describing these features of long-range interproton couplings have been published.^{7–10} The spin polarization of π electrons in a planar system was related to that produced by a hyperconjugative interaction, through the so-called “methyl group replacement rule” where $^nJ^\pi$ in the former is approximately equal to $-^{n+1}J^\pi$ in the corresponding benzylic coupling obtained replacing one of the coupled protons by a

CH_3 group.^{6,10} It is noteworthy that theoretical approaches that allow the decomposition of calculated coupling constants into σ - and π -transmitted components, such as the PRMO (partially restricted molecular orbitals)¹¹ and IPPP (inner projections of the polarization propagator)¹² approaches, reproduce quite closely the $a + b \times \sin^2 \theta$ dependence of the π component of benzylic couplings,¹³ where the signs of parameters a and b satisfy the alternating sign rule⁷ and θ is the dihedral angle defined by the side chain $\text{C}_\alpha-\text{H}$ bond and the aromatic ring plane. A similar trend has been found in calculated allylic couplings.¹⁴

The stereospecificity of the σ -transmitted component and the angular dependence of the component originated in a $\sigma \rightarrow \pi$ hyperconjugative interaction^{6,7} indicate that electron delocalizations are fundamental for transmitting the spin information associated to the Fermi contact interaction.⁸ These delocalizations are the base of Schaefer's “ J -method” to determine side-chain conformations when long-range J_{HH} couplings are accurately measured.¹⁵ Electron delocalizations are known to be stereospecific interactions, and Dewar and Dougherty have stressed their importance in σ -type orbitals,¹⁶ being of particular importance for vicinal σ -bonds in a trans arrangement.¹⁷

Among the current approaches to study electron delocalizations and stereoelectronic interactions, the natural bond orbital (NBO) method is one of the most appealing.¹⁸ Using this approach, Weinhold et al.^{19,20} showed the importance of certain electron delocalizations as to their contribution to several spin–spin coupling constants. Recently, several NBO-based meth-

* To whom correspondence should be addressed. Fax: 54-11-4576-3385. E-mail: burton@qo.fcen.uba.ar.

ologies have been used for dissecting Fermi contact contributions to scalar couplings. In one case, the contributions of different interactions to three-bond $^1\text{H}-^1\text{H}$ coupling constants were analyzed using a NBO-derived deletion method.²¹ On the other hand, the natural J -coupling (NJC) method decomposes the scalar coupling by describing the Fermi contact term using localized orbitals (NBOs),²² as a Lewis type (localized) contribution $J^{(L)}$ and two nonlocalized contributions $J^{(\text{deloc})}$ and $J^{(\text{repol})}$, the latter two arising from electron density transfer between donor and acceptor orbitals in different parts of the molecule and within a bond region, respectively. Another related method using NLMOs decomposes the Fermi contact term in orbital contributions.²³ Natural bond orbital parameters such as deletion and perturbative energies, orbital occupation numbers, and orbital energies have been used to analyze delocalization effects or hyperconjugative interactions in several cases.²⁴ When two nuclei experiment a non-null indirect coupling, several spin-polarization mechanisms^{25,26} can be envisioned based on stereoelectronic interactions.

In this work a new methodology for evaluating the contribution of the hyperconjugative interactions to three- and four-bond H–H coupling constants is presented. From a physical point of view, this allows the evaluation of the effect of nonlocalized contributions (similar to $J^{(\text{deloc})}$ and $J^{(\text{repol})}$ of the NJC method), although it is not restricted to the Fermi contact term, as other coupling terms as well as other properties may be obtained using the same formalism. An approach to the elucidation of some coupling mechanisms is made.

2. Methods and Details of the Calculations

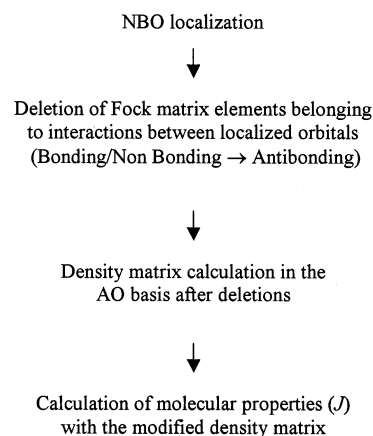
Geometry optimizations and NBO analysis were carried out with the Gaussian 98 package of programs,²⁷ and magnetic properties were calculated with the program SYSMO.²⁸ Optimized geometries were computed at the MP2/6-31G** level of theory. Single point calculations, including NBO analysis, were done at the RHF/6-31G** level of theory, except in the case of propene where the RHF/6-311G** basis set was used.

The dependence of couplings on angles is accepted to be dominated by the Fermi contact (FC) contribution, and it has been shown that trends can be reproduced using modest basis sets.²⁹ In our work, FC results obtained with the basis sets stated above reproduce satisfactorily experimental trends in all model compounds analyzed. Furthermore, as relative intensities of NBO deletion energies are not too sensitive to improvements in the basis set, the same basis was chosen for the present analysis.

In the model compounds used, a range of conformations were considered by varying dihedral angles θ in 30° or ca. 60° steps so as to have at least seven points in the entire interval, i.e., $0^\circ-180^\circ$ or $-180^\circ-+180^\circ$ depending on the symmetry. When treating structures out of the equilibrium geometry, the dihedral angle θ was taken fixed and the other degrees of freedom were allowed to relax. Full optimizations were performed using redundant internal coordinates, while restricted ones were done using Z-matrix coordinates.

Natural bond orbital (NBO) analysis were used to evaluate delocalization effects, and the calculations were performed using module 3.1³⁰ of the Gaussian 98 suite of programs. With the NBO deletion procedure, the energy of the orbital interaction of interest was evaluated by zeroing the corresponding off-diagonal Fock matrix elements and recalculating the molecular orbitals (and density matrix) as though the interaction was absent. With this modified density matrix the program evaluates a modified energy E' ; the difference between the total SCF energy (E) and E' gives the delocalization energy.

SCHEME 1



To evaluate the effects of stereoelectronic interactions over coupling constants, a methodology derived from the NBO deletion procedure was used (Scheme 1). Briefly, a natural bond order (NBO) localization was performed, followed by the deletion of selected off-diagonal Fock matrix elements written in the NBO basis, $\langle\sigma_m|\hat{F}|\sigma_n^*\rangle$ and $\langle\sigma_n^*|\hat{F}|\sigma_m\rangle$ representative of delocalization interactions between selected orbitals σ_m and σ_n^* , where σ and σ^* are used in a generic sense to refer to filled and unfilled orbitals of the formal Lewis structure, and \hat{F} stands for the Fock operator. The density matrix was then recalculated in the atomic orbital basis using the modified Fock matrix as though the interaction was absent. With this modified density matrix the electronic polarization propagator³¹ was calculated, with which in turn it is possible to obtain first and higher order properties, such as the magnetic couplings of interest in this work.

The Computational Procedure. In practice, the procedure to evaluate stereoelectronic contributions to molecular properties was implemented by means of a combination of several modules of the programs Gaussian 98 and SYSMO. To be able to implement the procedure of deletion of Fock matrix elements, a single point calculation was made, followed by a standard NBO localization procedure and the deletion of selected Fock matrix elements, using the Gaussian electronic structure package.

This procedure was recorded in a binary scratch file that included the density matrix modified by deletions. This file was then transformed into ASCII format and used as an input to SYSMO by means of an appropriate modification of its module 400.

To implement the procedure of deletions through the different modules of Gaussian 98, a nonstandard route was used. After definition of a usual route including basis set information, symmetry of the wave function and a SCF calculation, a NBO localization was made followed by a standard deletion procedure. Then, one step of a SCF optimization was carried out with the purpose of relaxing the wave function resulting from direct deletion and thus avoiding the molecular system being too far from a variational minimum. The complete procedure was recorded in a Gaussian scratch file, so the molecular orbital coefficients belonged to the modified wave function. Afterward, a series of modules of the SYSMO or Gaussian packages were used to calculate selected response properties, following the conventional procedure of each package.

The magnitudes calculated with the method described above were compared with the magnitudes obtained without deletions, thus allowing evaluation of the relative contributions of the interactions involved. With J being the value of the magnetic

coupling obtained with the complete Fock matrix and J' the calculated value with the deletions, in the ideal case the angular dependence of J' should disappear if the interactions deleted were those responsible for the angular variation of J , that is, $J' = C$, where C is a constant representing a residual value that does not vary with the dihedral angle θ . In the real case, a more complex relationship arises, which in a first-order approximation could be represented as $J' = \alpha J + C$. A nonzero value of α results because the deletion procedure does not cancel completely the interactions; thus a linear relationship between ΔJ and J should be maintained but the slope ($1 - \alpha$) will not be equal to 1. This linear relationship is indicative that the group of deleted interactions are sufficient to account for the angular dependence of spin density transfer. In this respect, ΔJ values for the deletion of individual interactions or selected combinations may be considered as being proportional to the contribution of those interactions to the coupling constant (see below).

The ΔJ values for the individual interactions were calculated in the angle range under study, and different combinations were tested (additively) searching for the minimal set of interactions that would show a good correlation coefficient for the linear relationship between ΔJ and J . The ΔJ calculation was then repeated with the simultaneous deletion of the selected interactions and the correlation coefficient was recalculated. In a strict sense, all interactions may contribute to a certain extent to the variation of J ; this methodology allows the identification of significant and negligible contributors.

3. Results and Discussion

The NBO-based method was applied to three different types of pathways connecting the coupled nuclei: saturated compounds, where the couplings are transmitted through σ bonds, using ethane and propane as model compounds (Figure 1a,b); unsaturated compounds, where couplings can be transmitted through the σ and π electronic systems, with propene (Figure 1c) as a model compound; cyclopropane derivatives where one of the C–C bonds of the cyclopropane moiety belongs to the coupling pathway. The high p character of the latter bonds is well-known;³² therefore, this coupling pathway may be considered of an intermediate character between the previous two. Methylcyclopropane (Figure 1d) was chosen as a model compound in this case.

The contribution of the different donor–acceptor delocalization interactions to the angle dependence of scalar couplings is related to the transfer of spin density from bonding to antibonding orbitals. However, the effect produced by delocalizations on energy-related properties differs from that produced on other properties such as the coupling constants analyzed in this work. The magnitude of the change in the coupling constants due to the deletion of delocalization interactions is proportional to the contribution of those interactions to the transfer of spin density between the coupled nuclei. This could be related by the overlap of the orbitals involved.²² For direct interactions between orbitals involving the coupled nuclei, interpretation is straightforward; however, for interactions not involving both coupled nuclei, it may be assumed that spin density is transferred by way of a network that includes all delocalization interactions in the molecule. As will be shown below, only pathways including localized orbitals with high s character (σ and σ^* orbitals) involving one of the coupled nuclei are important to explain angular dependence of the FC term of the coupling constants, because they have the greatest amplitude at the coupled nuclei. Interactions not involving the coupled nuclei

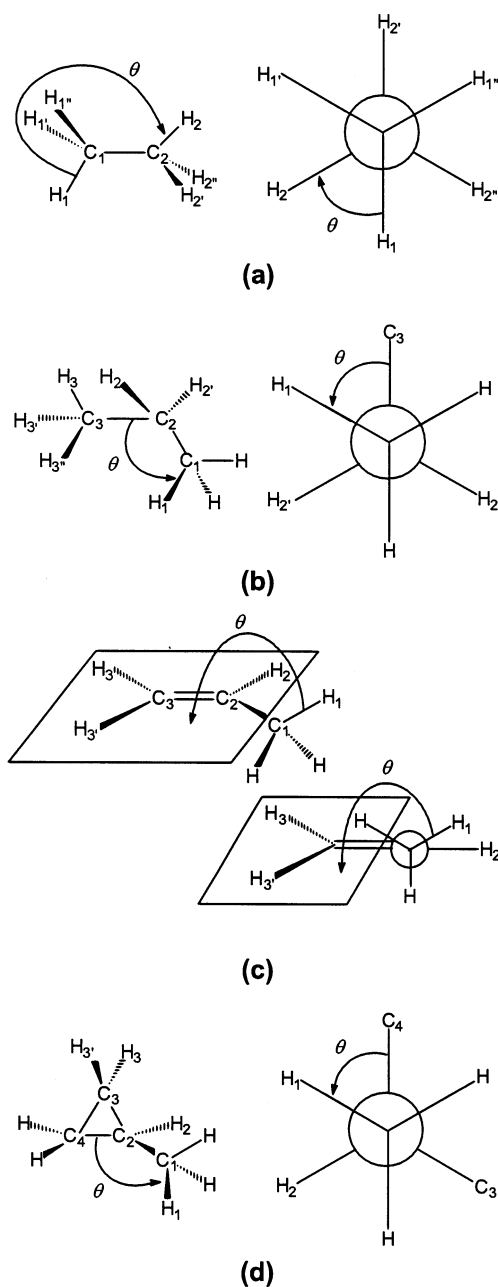


Figure 1. Atom numbering and dihedral angle definitions for the model compounds (a) ethane, (b) propane, (c) propene, and (d) methylcyclopropane

are relevant when they are part of the shortest geometrical path between them and involve a significant associated stabilization energy.

In this work, geminal interactions of the form $\sigma(C-C_i) \rightarrow \sigma^*(C_i-H_i)$ between a bonding $C-C_i$ sigma orbital and an antibonding C_i-H_i orbital (where H_i is one of the coupled hydrogens under consideration) are denoted by Gem_i . When both bonds include carbon atoms, i.e., $\sigma(C_1-C_2) \rightarrow \sigma^*(C_2-C_3)$, the notation Gem_C will be used. Notation Vic_i will be used to denote vicinal interactions of the form $\sigma(C-C_j) \rightarrow \sigma^*(C_i-H_i)$ for the case of four-bond couplings, where carbon atom C_j belonging to the $C-C$ bond is bonded to one of the coupled hydrogens under consideration (H_j) and H_i is the other coupled hydrogen. In the case of ethane, the only possible vicinal interactions are of the form $\sigma(C_j-H_j) \rightarrow \sigma^*(C_i-H_i)$, where H_j represents one of the coupled protons under consideration, and notation Vic_i will be used also in this case for the sake of simplicity. When

TABLE 1: Notation Used for Specific Interactions of Methylcyclopropane^a

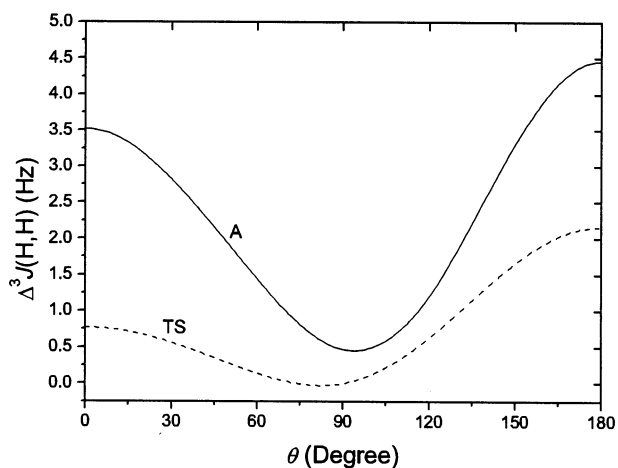
notation	interaction
Gem _C	$\sigma(\text{C}_2-\text{C}_3) \rightarrow \sigma^*(\text{C}_1-\text{C}_2)$
Gem _C ^R	$\sigma(\text{C}_1-\text{C}_2) \rightarrow \sigma^*(\text{C}_2-\text{C}_3)$
Vic ₂	$\sigma(\text{C}_3-\text{H}_3) \rightarrow \sigma^*(\text{C}_2-\text{H}_2)$
Vic ₂ ^R	$\sigma(\text{C}_2-\text{H}_2) \rightarrow \sigma^*(\text{C}_3-\text{H}_3)$
Vic ₂ '	$\sigma(\text{C}_3-\text{H}_3') \rightarrow \sigma^*(\text{C}_2-\text{H}_2)$
Vic ₂ ' ^R	$\sigma(\text{C}_2-\text{H}_2) \rightarrow \sigma^*(\text{C}_3-\text{H}_3')$
Vic ₄	$\sigma(\text{C}_2-\text{H}_2) \rightarrow \sigma^*(\text{C}_1-\text{H}_1)$
Vic ₄ ^R	$\sigma(\text{C}_1-\text{H}_1) \rightarrow \sigma^*(\text{C}_2-\text{H}_2)$
Vic ₅	$\sigma(\text{C}_2-\text{C}_4) \rightarrow \sigma^*(\text{C}_3-\text{H}_3)$
Vic ₅ ^R	$\sigma(\text{C}_3-\text{H}_3) \rightarrow \sigma^*(\text{C}_2-\text{C}_4)$
Vic ₅ '	$\sigma(\text{C}_2-\text{C}_4) \rightarrow \sigma^*(\text{C}_3-\text{H}_3')$
Vic ₅ ' ^R	$\sigma(\text{C}_3-\text{H}_3') \rightarrow \sigma^*(\text{C}_2-\text{C}_4)$
Vic ₆	$\sigma(\text{C}_2-\text{C}_4) \rightarrow \sigma^*(\text{C}_1-\text{H}_1)$
Vic ₆ ^R	$\sigma(\text{C}_1-\text{H}_1) \rightarrow \sigma^*(\text{C}_2-\text{C}_4)$

^a Interactions not listed follow the same notation rules used for propane.

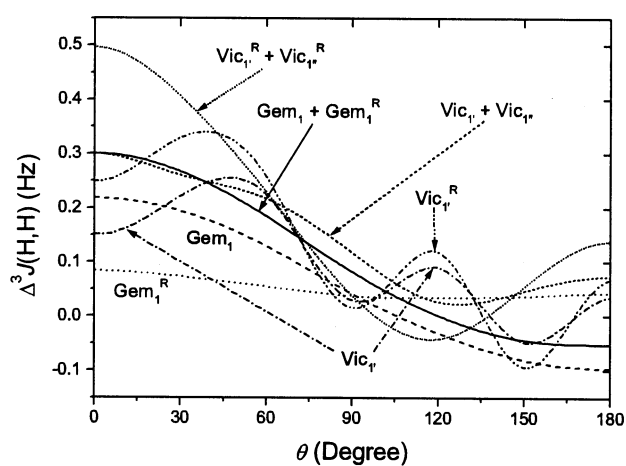
the reverse interactions are considered, $\sigma(\text{C}_i-\text{H}_i) \rightarrow \sigma^*(\text{C}_i-\text{C})$ or $\sigma(\text{C}_i-\text{H}_i) \rightarrow \sigma^*(\text{C}_j-\text{H}_j)/\sigma(\text{C}_i-\text{H}_i) \rightarrow \sigma^*(\text{C}-\text{C}_j)$, an “R” is added as a superscript (Gem_{*i*}^R and Vic_{*i*}^R, respectively). When a pi orbital needs to be considered, it is indicated explicitly, adding a π subscript (Gem_{*i*} ^{π} or Vic_{*i*} ^{π}). Direct, through-space interactions between bonds that include the coupled hydrogens are dubbed TS and TS^R. Additional notation is used for the case of methylcyclopropane as needed (Table 1). It should be noted that the same notation may indicate different interactions when different pairs of coupled hydrogens are considered, even within the same compound.

Three-Bond Coupling Constants. Ethane. The ethane molecule was used as a model compound for studying contributions to ^1H – ^1H three-bond coupling constants as a function of the dihedral angle θ (see Figure 1a for atom numbering and angle definition). Although related studies have been published recently for ethane,^{21,22} a more detailed analysis centered on the effect of delocalization interactions and their contribution to the angular dependence of 3J is presented here. Figure 2 shows the effect on the Fermi contact term between H₁ and H₂ upon deletion of individual interactions and of selected combinations. The through-space interaction TS ($\sigma(\text{C}_1-\text{H}_1) \rightarrow \sigma^*(\text{C}_2-\text{H}_2)$) involving the bonding and antibonding orbitals of the coupled hydrogens under consideration makes the overall major individual contribution, as shown previously.^{1,21,22} However, this contribution is negligible when the dihedral angle between the coupled hydrogens is close to 90° and is considerably more important for angles in the range 120°–180°, being practically the sole contributor at 180° (Figure 2a). Near the 0° dihedral, vicinal interactions between orbitals localized over the C–H bond involving the coupled hydrogens (H₁, H₂) with the bonding and antibonding orbitals involving the other hydrogens (H₁', H₁'', H₂', H₂''), and the geminal interactions with the C–C bond orbitals contribute in more or less equal proportions to the Fermi contact term (Figure 2b). Among these, it is noteworthy that the interactions that involve bonding orbitals of the coupled hydrogen under consideration are less important than those involving antibonding orbitals (compare Vic₁' with Vic₁'^R). This is probably due to the fact that J is a second order response property, its value being strongly dependent on the properties of the vacant orbitals through the occupied–vacant interactions in the polarization propagator.

It is interesting to compare the above results with those obtained with the NJC method.²² Thus, the term $J_{\text{vic}}^{\text{(deloc)}}$, which in our case corresponds to the sum of TS and TS^R, has numerical values very similar to those shown in Figure 2a. Good



(a)



(b)

Figure 2. Differences in coupling constants $\Delta^3J(\text{H}_1, \text{H}_2)$ resulting from deletion of relevant interactions for ethane as a function of the H₁–C₁–C₂–H₂ dihedral angle θ : (a) through-space interaction (TS) and combination of several interactions taken together (A = Gem₁ + Gem₁^R + Gem₂ + Gem₂^R + TS + TS^R + Vic₂ + Vic₂^R + Vic₂' + Vic₂'^R + Vic₁' + Vic₁'^R + Vic₁'' + Vic₁''^R) with a 0.994 correlation coefficient with calculated FC term; (b) other relevant interactions, including single delocalizations and relevant combinations from symmetry considerations. As a consequence of the symmetry of the molecule, the curves that correspond to interactions denoted with subscript 1 are the same as those with subscript 2. In addition, those interactions denoted with a double prime are the same as those denoted with a single prime, but shifted by 120°.

correlations were also obtained between ΔJ for the TS + TS^R interaction and the second-order energy lowering $E^{(2)}$ (which measures the energy associated with delocalizations) for the orbitals involved, in the ranges 0° < θ < 80° (correlation coefficient = 0.999) and 90° < θ < 180° (correlation coefficient = 1.000). These results suggest that our estimate of the contribution of delocalization effects to the Fermi contact term should be numerically equivalent to that resulting from the NJC method, considering the differences in methodologies and basis set used for calculation of the coupling constant.

The search for the best combination of interactions that linearly correlates ΔJ and J gives complementary information for the analysis of individual interactions. Several interactions may affect the couplings within an arbitrary dihedral interval, with different signs and intensities. The net effect of the combination of individual interactions determines the behavior of the coupling as a function of the dihedral angle.

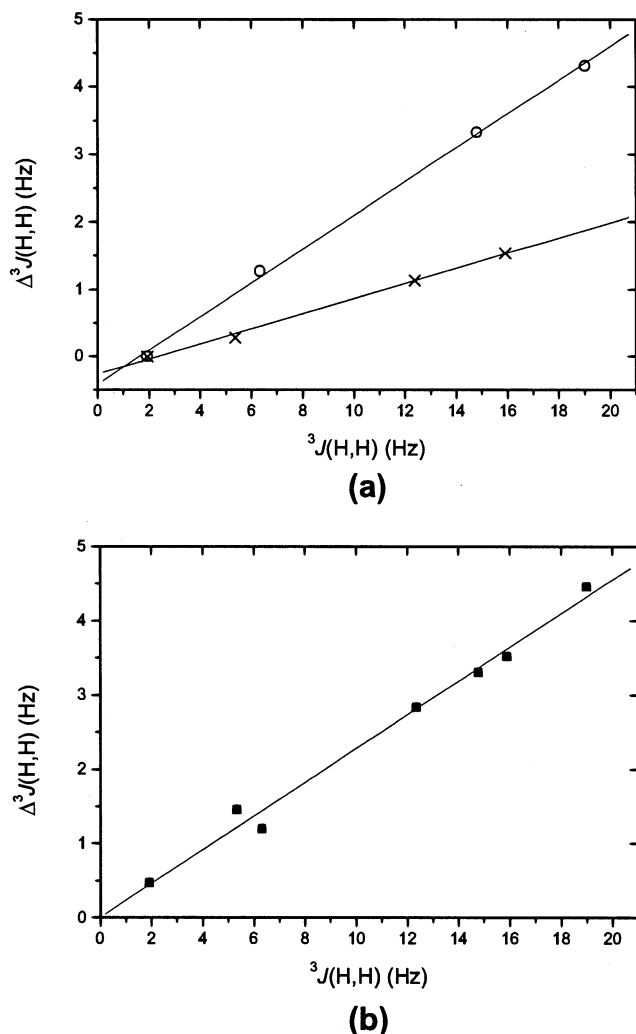


Figure 3. Differences in coupling constants $\Delta^3J(H_1, H_2)$ resulting from deletion of relevant interactions for ethane as a function of $^3J(H_1, H_2)$: (a) through-space interaction (TS + TS^R) in the ranges $0^\circ < \theta < 90^\circ$ (x) and $90^\circ < \theta < 180^\circ$ (O); (b) combination A in Figure 2a in the range $0^\circ < \theta < 180^\circ$ (correlation coefficient = 0.994, slope = 0.227 \pm 0.011).

The main interaction, namely TS, does not give a good correlation over the whole interval 0° – 180° , although good correlations are evident in the smaller ranges 90° – 180° and 0° – 90° (Figure 3a). As a consequence of this behavior, it is evident that other interactions that contribute to more positive couplings in the range 0° – 90° than in the range 90° – 180° need to be considered. Moreover, these interactions should be more intense near $\theta = 0^\circ$ than $\theta = 90^\circ$. A good correlation for the complete range 0° – 180° may be obtained when several interactions are taken jointly; thus the combined deletions (indicated as “A” in Figure 2a) follow very well the angular dependence of 3J with an excellent linear relationship between ΔJ and J (Figure 3b, correlation coefficient = 0.994).

Deletion energies were also calculated corresponding to the combination of interactions that best fit the relation Δ^3J_{HH} vs $^3J_{HH}$, i.e., combination A, as a function of the dihedral angle θ . The correlation of these values with the corresponding FC term is poor (correlation coefficient = 0.653), suggesting that deletion energies corresponding to combination of deletions do not properly reproduce the effect of a combination of interactions over the couplings.

Four-Bond Coupling Constants. Propane. The propane molecule was used as the model compound for studying

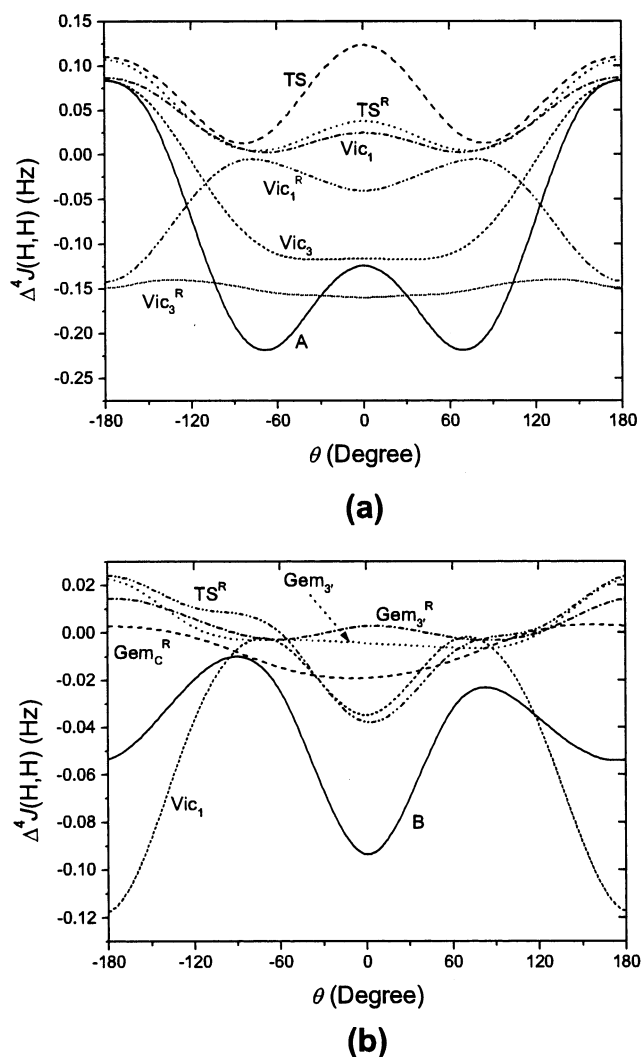


Figure 4. Differences in coupling constants resulting from deletion of relevant interactions for propane as a function of the $H_1-C_1-C_2-C_3$ dihedral angle θ : (a) $\Delta^4J(H_1, H_3)$, curve labeled A shows the behavior of the shown individual interactions taken together (A = TS + TS^R + Vic₁ + Vic₁^R + Vic₃ + Vic₃^R) with a 0.977 correlation coefficient with the calculated FC term (slope = 0.095 \pm 0.009); (b) $\Delta^4J(H_1, H_3)$, curve labeled B shows the behavior of the shown individual interactions taken together (B = Gem_C^R + Gem₃ + Gem₃^R + Vic₁ + TS^R) with a 0.968 correlation coefficient with the calculated FC term (slope = 0.204 \pm 0.023).

contributions to 1H – 1H four-bond coupling constants through σ bonds, as a function of dihedral angles (see Figure 1b for atom numbering and angle definitions). Figure 4 shows the relevant interactions that contribute to $^4J(H_1, H_3)$, corresponding to the anti arrangement of the C_1-C_2 and C_3-H_3 bonds ($C_1-C_2-C_3-H_3$ angle = 180°), and $^4J(H_1, H_3)$, which corresponds to the gauche relationship between the C_1-C_2 and C_3-H_3' bonds ($C_1-C_2-C_3-H_3'$ angle ca. -60° (-59.7°)). Geminal interactions (Gem) involve orbitals of both $C-C/H$ and $C-C/C$ bond pairs (only the first are significant), and vicinal interactions (Vic) correspond to $C-C/H$ pairs; in this case only $C-H$ bonds involving the coupled H's make significant contributions. For H_3 , which lies in the plane defined by $C_1-C_2-C_3$, the differences observed in the Fermi contact term upon deletion of significant interactions and of selected combinations are shown in Figure 4a. Due to molecular symmetry the curve is symmetrical with respect to $\theta = 0^\circ$; hence, the following analysis will refer only to the positive values of θ . The direct interactions involving bonding and

antibonding orbitals of the coupled H's (TS and TS^{R}) contribute to a positive coupling constant mainly at angles θ close to 0° and 180° and are negligible near 90° . As a consequence of dihedral rotation around the C_1 - C_2 bond, C_1 - H_1 geometrically differs from C_3 - H_3 , and due to this reason the $\sigma(\text{C}_1-\text{H}_1) \rightarrow \sigma^*(\text{C}_3-\text{H}_3)$ interaction (TS) has comparable effects in θ ranges above and below 90° , while the reverse $\sigma(\text{C}_3-\text{H}_3) \rightarrow \sigma^*(\text{C}_1-\text{H}_1)$ (TS^{R}) is more important only in the 120° - 180° range. The vicinal interactions $\sigma(\text{C}_1-\text{C}_2) \rightarrow \sigma^*(\text{C}_3-\text{H}_3)$ and $\sigma(\text{C}_3-\text{H}_3) \rightarrow \sigma^*(\text{C}_1-\text{C}_2)$ (Vic_3 and Vic_3^{R}) are the major contributors to the negative values of 4J , and Vic_3 is the main individual contribution to the asymmetry observed between the two maxima at 0° and 180° . It should be noted that Vic_3^{R} is practically insensitive to the change in θ . Other major contributors at the 180° angle, which corresponds to the "W" arrangement and the largest positive value of 4J , are the vicinal interactions $\sigma(\text{C}-\text{C}) \rightarrow \sigma^*(\text{C}-\text{H})$, i.e., Vic_1 and Vic_3 . Geminal interactions $\sigma(\text{C}-\text{C}) \rightarrow \sigma^*(\text{C}-\text{H})$ (not shown in the figure) diminish the value of 4J . For the 0° angle relationship a negligible coupling results due to the opposed effects of several interactions which compensate.

To account for the overall angular variation of 4J , the best combination of interactions indicated as "A" involves both direct interactions (TS and TS^{R}) and vicinal interactions Vic_1 , Vic_1^{R} , Vic_3 , and Vic_3^{R} (correlation coefficient = 0.977). This indicates that spin density transfer takes place by way of the most intense interactions involving orbitals of H_1 and H_3 , through the shortest geometrical path between both hydrogens.

Figure 4b shows the contributions to the four-bond coupling constant for a C_1 - C_2 - C_3 -H dihedral angle, ca. -60° , which corresponds to $^4J(\text{H}_1, \text{H}_3)$. In this case, the vicinal interaction Vic_1 , $\sigma(\text{C}_2-\text{C}_3) \rightarrow \sigma^*(\text{C}_1-\text{H}_1)$, appears as the most important interaction contributing to negative couplings, specially in the range $120^\circ < \theta < 240^\circ$ and around $\theta = 0^\circ$. For the other θ values, its contribution is almost negligible. Comparison of this interaction with the tendency shown by the coupling constant (which closely follows curve B, Figure 4b), shows that the relative contribution of Vic_1 to the minimum at 180° with respect to the minimum at 0° is greater than necessary in order to interpret the variation of the couplings upon dihedral angle variation. Important contributors to more negative couplings at 0° are the direct interaction TS^{R} and, to a lesser extent, the geminal interaction Gem_C^{R} . These contributions tend to equalize the minima at 180° and 0° with respect to the contribution of interaction Vic_1 considered alone. On the other hand, interactions Gem_3 and Gem_3^{R} contribute to more positive couplings, especially at θ values near 180° . TS^{R} is also an important contributor to more positive couplings near 180° . The net effect of these interactions taken together is enough to account for the overall angular variation of $^4J(\text{H}_1, \text{H}_3)$, as shown in curve B of Figure 4b (correlation coefficient = 0.968).

It is noteworthy that TS^{R} and Vic_1 are important contributors to both $^4J(\text{H}_1, \text{H}_3)$ and $^4J(\text{H}_1, \text{H}_3')$ as the part of the molecule involved is geometrically equivalent in both cases. However, interaction Vic_3 , which in the case of H_3 corresponds to a geometry in which the interacting orbitals are in an anti orientation and is thus important, is replaced in the case of H_3' by a combination of geminal interactions involving H_3' , in the coupling pathway between the corresponding hydrogens ($\text{Gem}_C^{\text{R}} + \text{Gem}_3' + \text{Gem}_3^{\text{R}}$). Although the relative geometry of atom pairs involved in some of the interactions discussed remains unchanged upon rotation of the dihedral θ , their contribution is still significant. This sensitivity to angle variation is probably due to the interaction of mobile orbitals belonging to the C_1 -

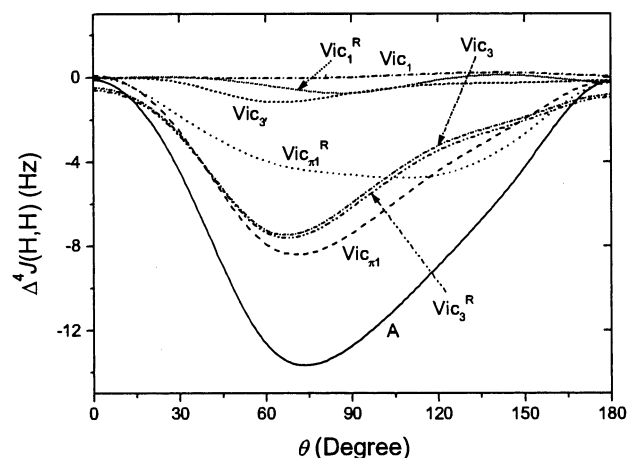


Figure 5. Differences in coupling constants $\Delta^4J(\text{H}_1, \text{H}_3')$ (cisoid), resulting from deletion of relevant interactions for propene as a function of the H_1 - C_1 - C_2 - C_3 dihedral angle θ . Curve labeled A shows the behavior of several interactions taken together ($A = \text{Vic}_1 + \text{Vic}_1^{\text{R}} + \text{Vic}_3 + \text{Vic}_3^{\text{R}}$) with correlation coefficient with the calculated FC term of 0.996 (slope = 0.218 ± 0.011).

H_1 bond that interact with other orbitals. These may be distorted in such a way that their interactions with other orbitals are also affected.

Propene. In the case of the allylic coupling, as in propene (see Figure 1c for angle definition and atom numbering), the π system introduces a clear difference from the previous case. Instabilities of the wave function were avoided using an improved basis set (RHF/6-311G**) in the calculations. However, a small positive eigenvalue of the polarization propagator resulted, causing an overestimation of the π contribution. Despite the above, experimental tendencies are qualitatively satisfied as shown for the case of the coupling constants corresponding to the cisoid proton H_3' , which closely follows curve A in Figure 5.³⁴

For allylic couplings, a clear distinction appeared between σ - and π -transmitted components $^4J_{\text{H,H}} = ^4J_{\text{H,H}}(\sigma) + ^4J_{\text{H,H}}(\pi)$. The former follows a trend similar to that of the four-bond couplings transmitted through a saturated coupling pathway⁷ and is affected by the same type of interactions as those found above for propane. Considering that the most pronounced features of allylic couplings may be rationalized in terms of a π -electron mechanism,³³ the π contribution to $^4J_{\text{H,H}}$ couplings in propene fragments was analyzed, although conclusions should be treated with care especially when considering the relative contribution of the σ path. In propane, in the case of H_3 (anti), the role of several vicinal interactions is crucial for interpreting the angular dependence of the coupling, and many of them are more intense than those relevant for the case of H_3' . Thus it may be inferred that the relative contributions of these σ interactions to the coupling constant of the transoid proton in propene (H_3 , geometrically equivalent to the propanic anti H) are more important than for the case of the cisoid proton (H_3'). In view of the above, only the cisoid proton will be considered in detail within the analysis of ΔJ , where the π contribution to the coupling is significantly more important than the σ contribution.

For the 4J coupling between H_1 and the cisoid H_3' , one of the major contributions to the negative value in the 30° - 150° range of θ comes from the vicinal $\pi(\text{C}_2-\text{C}_3) \rightarrow \sigma^*(\text{C}_1-\text{H}_1)$ interaction and in a somewhat lesser extent from the reverse $\sigma(\text{C}_1-\text{H}_1) \rightarrow \pi^*(\text{C}_2-\text{C}_3)$ ($\text{Vic}_{\pi 1}$ and $\text{Vic}_{\pi 1}^{\text{R}}$, Figure 5). These interactions do not contribute significantly at 0° and 180° .

Additional contributions for the complete range of θ values originate in the vicinal interactions Vic_1 , Vic_1^{R} , and Vic_3 . Important contributions from interactions involving $\text{C}_1\text{--C}_2$ σ bonds and antibonds, namely Vic_3 and Vic_3^{R} , compensate with other interactions (not shown).

Excellent correlations for the angular dependence of 4J corresponding to transoid and cisoid H's result from interaction $\pi(\text{C}_2\text{--C}_3) \rightarrow \sigma^*(\text{C}_1\text{--H}_1)$ (correlation coefficient = 0.994 in both cases). Interactions that combine σ and π contributions between $\text{C}_2=\text{C}_3$ and $\text{C}_1\text{--H}_1$ bonds, indicated as "A" in Figure 5, show a slight improvement in the correlation coefficient, namely 0.994 for the transoid and 0.996 for the cisoid. The addition of vicinal interactions Vic_3 and Vic_3^{R} , which will be named combination B, improves again slightly the correlation in the transoid case (0.995), while the addition of Vic_3' and $\text{Vic}_3'^{\text{R}}$ (combination C) deteriorates slightly the correlation in the cisoid case (0.995). These schemes are similar to scheme A in propane, as they include vicinal interactions that involve the coupled protons under consideration.

As discussed previously, one of the most important features of the formalism of deletions is to explain the tendency followed by coupling constants upon variation of dihedral angles. For this purpose, correlations between calculated couplings (J) and their variations produced by deletions (ΔJ) were calculated. However, in the case of propene several combinations of interactions give rise to very good correlation coefficients. To determine the combination of interactions that better explains tendencies of experimental and calculated coupling constants, differences between cisoid and transoid couplings were analyzed in more detail.

Combinations B and C for the transoid and cisoid cases, respectively (see above), include interactions that involve orbitals adjacent to both coupled protons, as is the case for the best combinations in propane (curves A and B, Figure 4) and in ethane (curve A, Figure 2). However, the differences ΔJ toward negative coupling constants due to these deletion schemes are larger for the transoid than for the cisoid proton, contrary to the trend shown by calculated and experimental values of 4J .³⁴ This may be due to the fact that in the transoid case combination B includes interactions Vic_3 and Vic_3^{R} , while in the cisoid case combination C includes Vic_3' and $\text{Vic}_3'^{\text{R}}$. As the $\text{C}_3\text{--H}_3$ bond is anti to $\text{C}_1\text{--C}_2$ while the $\text{C}_3\text{--H}_3'$ bond is syn, the magnitude of the stereoelectronic interaction is greater in the former, giving rise to a greater difference in ΔJ toward negative couplings. On the other hand, combination A gives larger differences in ΔJ in the cisoid than in the transoid case, making cisoid couplings more negative than transoid ones, in accordance with the trend showed by the calculated and experimental values.³⁴

To further clarify the role of the σ -path contributions to long-range couplings in propane and propene, a comparative analysis follows. In the conformations analyzed in both compounds, interactions Vic_3' and Vic_3 and the corresponding reverse interactions contribute significantly to negative values of the coupling constants (Figures 4 and 5, not shown in the gauche case in propane) except in the case of the H_3 in propane, where Vic_3 contributes to positive couplings for dihedral angles over 150° , near the "W" arrangement (Figure 4a). The other important vicinal interactions, $\text{Vic}_1 + \text{Vic}_1^{\text{R}}$, are either positive or oscillate around zero for conformations where the $\text{C}_1\text{--C}_2\text{--C}_3\text{--H}$ angles are 0° and 180° , i.e., in the case of the cisoid H_3' (Figure 5) and the transoid H_3 proton in propene (not shown) and the anti H_3 proton in propane (Figure 4a). In the case of H_3' in propane ($\text{C}_1\text{--C}_2\text{--C}_3\text{--H}_3'$ angle ca. -60°), these interactions contribute toward negative coupling constants. In summary, it is possible

to visualize a σ path that is common to both compounds. When the $\text{C}_1\text{--C}_2\text{--C}_3\text{--H}$ moiety is near the anti and syn conformations, vicinal interactions Vic_1 and Vic_1^{R} are of minor importance and are either positive or oscillate around zero, while for other $\text{C}_1\text{--C}_2\text{--C}_3\text{--H}$ angles their contributions are toward negative couplings. On the other hand, Vic_3 , Vic_3' , and their reverses always contribute toward negative couplings except for Vic_3 in the case of the "W" arrangement.

Methylcyclopropane. As mentioned above, the cyclopropane ring with its partial π character may be considered as an intermediate case between propane and propene. However, the analysis is more complex due to the larger number of bonding and antibonding orbitals that contribute significantly to the 4J couplings between H_1 and the anti and syn cyclopropyl protons, H_3 and H_3' , respectively (see Figure 1d for numbering and angle definitions). As in the previous cases, the calculated Fermi contact terms reproduce the experimental tendencies of the mentioned coupling constants.³²

Due to the large number of interactions that need to be considered, a special notation is required in the case of methylcyclopropane. The nomenclature used for interactions that do not follow the general rules stated above is summarized in Table 1.

At variance with all the cases previously analyzed, in the case of the anti cyclopropyl H there is not a unique set of interactions that can account for the overall angular variation of 4J . It is possible, however, to find different sets for the partially overlapping ranges $-180^\circ < \theta < 50^\circ$ and $-70^\circ < \theta < 180^\circ$, suggesting that small contributions from a large number of interactions add up to shape the overall angular variation. For the first range, the major contributors are the vicinal interactions of the bonding and antibonding $\text{C}_3\text{--H}_3$ orbitals with the $\text{C}_1\text{--C}_2$ orbitals (Vic_3 and Vic_3^{R}) and the interaction $\sigma(\text{C}_2\text{--C}_4) \rightarrow \sigma^*(\text{C}_3\text{--H}_3)$ (Vic_5); their combination is indicated as "A" in Figure 6a, with a correlation coefficient of 0.990. The individual interactions have opposite effects on the couplings; the former decrease the coupling constant while the latter increases it. It should be noted that, in the negative range of θ , the pair $\text{Vic}_3 + \text{Vic}_3^{\text{R}}$ prevails, while Vic_5 is more important in the positive range, resulting in a positive coupling for angles greater than approximately 40° . For the range $-70^\circ < \theta < 180^\circ$, combination B (Figure 6b), which includes the vicinal interaction of the bonding and antibonding $\text{C}_3\text{--H}_3$ (anti) orbitals with $\text{C}_2\text{--C}_1$ (Vic_3 , Vic_3^{R}) and the direct interaction of orbitals $\text{C}_3\text{--H}_3$ with $\text{C}_1\text{--H}_1$ (TS, TS^{R}), gives a good correlation coefficient (0.986). Although Vic_5 has a significant contribution in this range it is not included in combination B, suggesting that its effect in the angular variation of the coupling constant is compensated by other interactions. From a geometric point of view, for angles in the range $40^\circ < \theta < 130^\circ$, $\text{C}_3\text{--H}_3$ (anti) and $\text{C}_1\text{--H}_1$ acquire an orientation that resembles the "W" arrangement. In this range, interaction Vic_3 contributes to more positive couplings, and the combined effect of this interaction and $\text{TS} + \text{TS}^{\text{R}}$ gives rise to positive values of the couplings. The relevance of the direct $\sigma(\text{C--H}) \rightarrow \sigma^*(\text{C--H})$ interaction and the positive value of the Fermi contact term are propane-like characteristics.

For the syn cyclopropyl H (Figure 7), the major contributions come from the vicinal interactions involving bond and antibond orbitals of $\text{C}_1\text{--H}_1$ and $\text{C}_3\text{--H}_3'$ (syn) bonds and from the geminal interactions involved in the shortest bond path connecting both hydrogens. The main interactions are Vic_1 and Vic_1^{R} ($\sigma(\text{C}_2\text{--C}_3) \rightarrow \sigma^*(\text{C}_1\text{--H}_1)$ and $\sigma(\text{C}_1\text{--H}_1) \rightarrow \sigma^*(\text{C}_2\text{--C}_3)$), with a greater strength in the range $0^\circ < \theta < 180^\circ$, which includes those conformations in which H_1 does not eclipse the cyclopropane

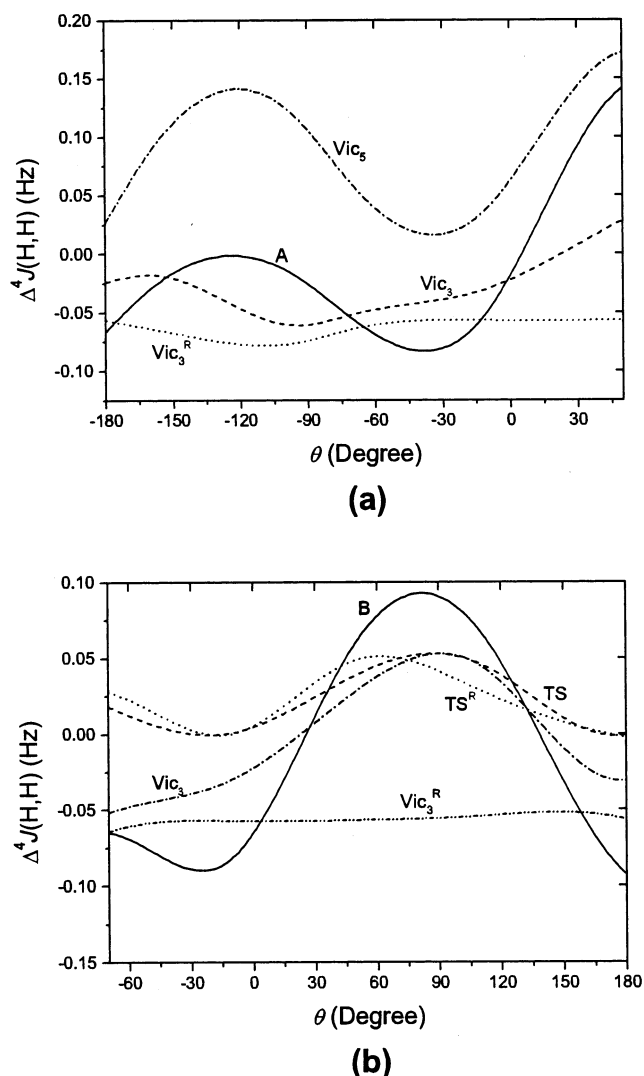


Figure 6. Differences in coupling constants $\Delta^4 J(\text{H}_1, \text{H}_3)$ (anti) resulting from deletion of relevant interactions for methylcyclopropane as a function of the $\text{H}_1-\text{C}_1-\text{C}_2-\text{C}_3$ dihedral angle θ : (a) dihedral interval $-180^\circ < \theta < 50^\circ$, curve labeled A shows the behavior of several interactions taken together, $A = \text{Vic}_3 + \text{Vic}_3^R + \text{Vic}_5 + \text{Vic}_5^R$, with correlation coefficient with the calculated FC term of 0.990 (slope = 0.287 ± 0.024); (b) dihedral interval $-70^\circ < \theta < 180^\circ$, curve labeled B shows the behavior of several interactions taken together, $B = \text{Vic}_3 + \text{Vic}_3^R + \text{TS} + \text{TS}^R$, with correlation coefficient with the calculated FC term of 0.986 (slope = 0.188 ± 0.018).

ring, i.e., according to the angle definition, angles lying outside the range $-70^\circ < \theta < 0^\circ$ (Figure 7a). As a consequence of the influence of Vic_1 and its reverse interaction, the minimum around $\theta = 70^\circ$ is deeper than the one corresponding to approximately $\theta = -100^\circ$.

The direct interaction between both C-H bonds is a small but significant contribution specially in the range $60^\circ < \theta < 120^\circ$ (Figure 7b). Vicinal interactions that involve the C_3-H_3 bond orbitals are minor contributors, the contribution of $\text{Vic}_2 + \text{Vic}_2^R$ to more negative coupling constants being more important in the angle intervals $-70^\circ < \theta < 0^\circ$ and $120^\circ < \theta < 180^\circ$ (Figure 7b), while $\text{Vic}_5 + \text{Vic}_5^R$ contribute to more positive coupling constants in the negative interval of θ and to more negative ones in the positive interval (Figure 7c). Vic_3 and Vic_3^R are slightly more important in the $150^\circ < \theta < 210^\circ$ angle interval and are approximately constant throughout the other values of θ (Figure 7b). With respect to interactions other than Vic_1 and Vic_1^R that involve bond and antibond C_1-H_1

orbitals with other vicinal bonds C_2-C_4 (Vic_6 and Vic_6^R) and C_2-H_2 (Vic_4 and Vic_4^R), interaction Vic_4 prevails in the range $-70^\circ < \theta < 0^\circ$, while Vic_4^R , Vic_6 , and Vic_6^R are smaller (Figure 7c). Geminal interactions involved in the shortest bond path connecting both hydrogens have similar qualitative behavior, being more intense in the angle interval $90^\circ < \theta < 270^\circ$ (Figure 7d).

The comparison of the coupling constants corresponding to anti and syn cyclopropyl protons shows that the former has common features with the propanic H_3 , while the latter has similarities with the propanic gauche and the propenic cisoid H couplings. In both anti cases (Figures 4a and 6) the main contributors to the absolute maxima of the coupling constants observed in propane and methylcyclopropane are the interactions TS , TS^R , and Vic_3 . In addition, in both model compounds a change of sign in the coupling constant takes place. With respect to the role of Vic_3 and Vic_3^R interactions, Vic_3^R has a fairly uniform contribution in both cases, while the added effects of Vic_3 and Vic_3^R are more important than $\text{Vic}_1 + \text{Vic}_1^R$.

On the other hand, in the gauche (propane) and syn (methylcyclopropane) cases, the interactions Vic_1 and Vic_1^R are the most significant (Figures 4b and 7). In these cases, the positions of the minima of the curve $\Delta^4 J(\text{H}, \text{H})$ vs θ , which follows closely curve B, Figure 4b and curve A, Figure 7a, respectively, come predominately from the effect of these interactions. For H_3 in propane they are at $\theta = 0^\circ$ and 180° , while in methylcyclopropane, the geometrically equivalent angle is the one defined by the $\text{H}_1-\text{C}_1-\text{C}_2-\text{C}_3$ dihedral, giving equivalent values of the θ angle that are approximately at -70° and 110° . An equivalent behavior is observed in the case of the maxima of $\Delta^4 J(\text{H}, \text{H})$.

With respect to the intensities of these extremes, the effect of Vic_1 and Vic_1^R interactions on the coupling constant ($\Delta^4 J_{\text{H}, \text{H}}$) of the syn H of methylcyclopropane and gauche H of propane is of similar magnitude for the two maxima but of different magnitude for the two minima. Consistently, curves B in Figure 4 and A in Figure 7a show maxima with similar intensities for both model compounds originating mainly in the mentioned Vic_1 and Vic_1^R interactions and minima with different intensities in the case of the gauche proton of propane (curve B, Figure 4b). However, a different behavior is observed in the case of the syn proton of methylcyclopropane, where the minima are of similar magnitude. This special behavior appears to originate in the concerted action of several small interactions. Minima of similar magnitude are also observed for the cisoid proton of propene, in this case due to the effect of vicinal interactions that involve π orbitals.

Some similarities between the cyclopropyl H_3 (syn) and the cisoid proton in propene could be based on the fact that the C_2-C_3 cyclopropane bond behaves in some situations like a double bond.³² As discussed above, the most significant contribution to $\Delta^4 J_{\text{HH}}$ in propene corresponds to vicinal interactions that involve the double bond. In a similar way, for the cyclopropyl H_3 (syn) the vicinal interactions that involve the cyclopropyl C_2-C_3 bond, Vic_1 and Vic_1^R , are the most important contributions to the variation of the coupling upon rotation of the dihedral angle θ . Moreover, a combination of interactions including vicinal interactions that involve the mobile (in the sense of θ angle rotation) methyl C_1-H_1 orbitals (curve A, Figure 7a), gives a good correlation (0.984) as in the case of cisoid couplings. The addition of vicinal interactions including $\text{C}-\text{H}_3$ (syn) orbitals ($A + \text{Vic}_2 + \text{Vic}_2^R + \text{Vic}_3 + \text{Vic}_3^R + \text{Vic}_5 + \text{Vic}_5^R$) deteriorates the correlation (correlation coefficient = 0.970), in a way similar to combination C for the cisoid H of propene. Combination A includes all geminal interactions

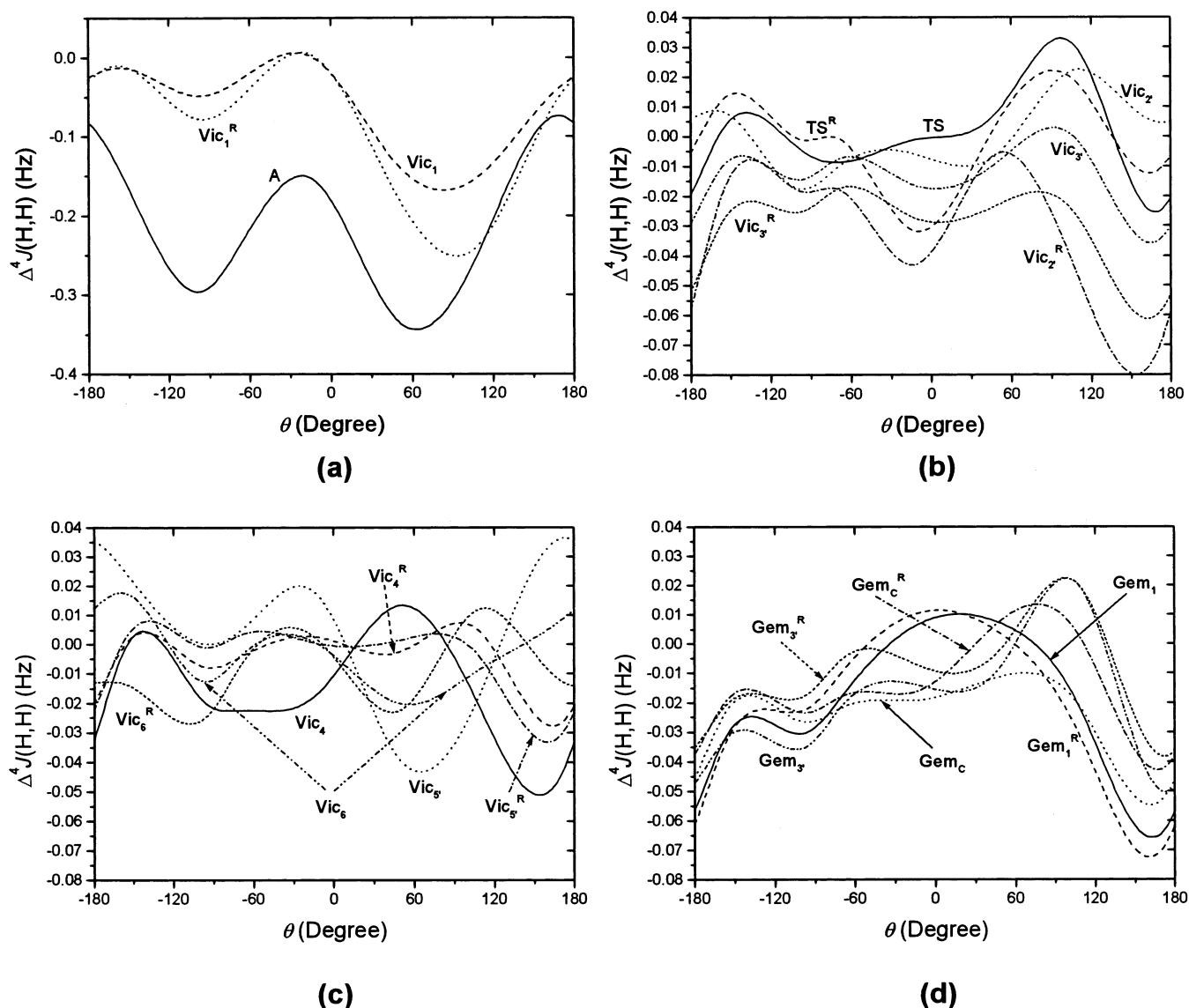


Figure 7. Differences in coupling constants $\Delta^4 J(H_1, H_3)$ (syn) resulting from deletion of relevant interactions for methylcyclopropane as a function of the $H_1-C_1-C_2-C_3$ dihedral angle θ : (a) vicinal interactions Vic_1 and Vic_1^R and the behavior of several interactions taken together ($A = Gem_1 + Gem_1^R + Gem_C + Gem_C^R + Gem_{3'} + Gem_{3'}^R + TS + TS^R + Vic_1 + Vic_1^R + Vic_4 + Vic_4^R + Vic_6 + Vic_6^R$) with correlation coefficient with the calculated FC term of 0.984 (slope = 0.186 ± 0.015); (b) through-space interactions and vicinal interactions Vic_2^R , Vic_2 , Vic_3^R , and Vic_3 ; (c) the remaining vicinal interactions; (d) geminal interactions.

that connect the coupled nuclei as well as the direct interaction and vicinal interactions mentioned above; as in propane, vicinal interactions are important only for certain relative orientations of the orbitals, for other geometries the transfer of spin density is mediated by a combination of geminal interactions.

Other similarities between anti protons arise from the asymmetry of the curves of the coupling constants vs dihedral angle: in the anti case the asymmetry between two consecutive maxima (curves A and B, Figure 6) is greater than for the syn case (curve A, Figure 7a). The same is observed when comparing the curve corresponding to H_3 in propane (curve A, Figure 4a) with those of the gauche $H_{3'}$ in propane (curve B, Figure 4b) and the cisoid $H_{3'}$ in propene (curve A, Figure 5).

4. Summary and Conclusions

In this work we presented a methodology for studying the variation of magnetic couplings between protons, upon deletion of selected stereoelectronic interactions. The method is rigorous from a formal point of view and gives a quantitative measure

of the relative contributions of stereoelectronic interactions to the molecular property, despite the fact that the NBO deletion procedure does not completely cancel the interactions. The additivity property is particularly useful as interactions may be analyzed on an individual basis, thus simplifying the overall procedure and allowing the straightforward prediction of combinations of interactions involved in the process under study. The method works well with systems containing both σ and π bonds, and even in systems with partial π character as cyclopropane rings. In the case of ethane, the through-space interaction between orbitals that involve the coupled protons is the most important contribution; however, the consideration of the other interactions is crucial in order to interpret the overall behavior of the $^3 J_{HH}$ coupling constant upon dihedral rotation. In the case of $^4 J_{HH}$ couplings, the comparison of the results shows that propane and propene have only a few interactions that contribute significantly to the couplings between protons. Specifically, the roles of vicinal and through-space interactions that include orbitals involving the coupled protons are very

important in the case of propane. In the case of propene, vicinal interactions that involve the π orbitals are, by far, the most important contributions. From a comparative analysis of propane and propene, it is possible to visualize a σ path common to both compounds, where vicinal interactions contribute either toward positive couplings (when the C_1 – C_2 – C_3 – H moiety is near anti and syn conformations, or to the “W” arrangement) or toward negative ones. In the model that contains a cyclopropyl ring, there are no unique interactions that influence the couplings, especially in the negative range of θ . In this case, the addition of several interactions gives rise to a behavior that may be interpreted as σ - and π -like mechanisms.

As a whole, it is clear that the path of delocalization interactions that significantly contributes to the transfer of spin density between coupled nuclei three and four bonds apart includes mainly vicinal and direct interactions. Among the former, those in which the interacting orbitals are close to the antiperiplanar orientation are favored. When the geometry departs significantly from this orientation, the transfer of spin density mediated by geminal interactions that include orbitals of the coupled hydrogens together with other geminal interactions in the shortest geometric path between them increases its relative contribution to the couplings.

Furthermore, the formalism used in this work can be extended to other response properties that depend on electronic excitation terms.

Acknowledgment. We thank CONICET (Argentina) and Universidad de Buenos Aires for financial support. E.M.S. thanks Universidad de Buenos Aires for a fellowship.

References and Notes

- (1) A preliminary account of this work was presented at the 12th National Symposium of Organic Chemistry (XII SINAQO), Los Cocos, Argentina, November 1999. Abstract published in *Molecules* [online computer file] **2000**, 5, 539.
- (2) Pople, J. A.; Schneider, W. G.; Bernstein, H. J. *High-Resolution NMR*; McGraw-Hill: New York, 1959.
- (3) Ramsey, N. F. *Phys. Rev.* **1953**, 91, 303.
- (4) (a) Lemieux, R. U.; Kullnig, R. K.; Bernstein, H. J.; Schneider, W. G. *J. Am. Chem. Soc.* **1957**, 79, 1005. (b) Karplus, M. *J. Chem. Phys.* **1959**, 30, 11.
- (5) McConnell, H. M. *J. Mol. Spectrosc.* **1957**, 1, 11.
- (6) Hoffman, R. A. *Mol. Phys.* **1958**, 1, 326.
- (7) Barfield, M.; Chakrabarti, B. *Chem. Rev.* **1969**, 69, 757.
- (8) Murrel, J. N. *Prog. NMR Spectrosc.* **1970**, 6, 1.
- (9) Günther, H.; Jikeli, G. *Chem. Rev.* **1977**, 77, 599.
- (10) Kowalewski, J. *Prog. NMR Spectrosc.* **1977**, 11, 1.
- (11) Engelmann, R.; Facelli, J. C.; Contreras, R. H. *Theor. Chim. Acta* **1981**, 59, 17.
- (12) Engelmann, R.; Contreras, R. H. *Int. J. Quantum Chem.* **1983**, 23, 1033.
- (13) Contreras, R. H.; Natiello, M. A.; Scuseria, G. E. *Magn. Reson. Rev.* **1985**, 9, 239.
- (14) Contreras, R. H.; Ruiz de Azúa, M. C.; Giribet, C. G.; Ferraro, M. B.; Diz, A. C. In *Nuevas Tendencias—Química Teórica*; Fraga, S., Ed.; CSIC: Madrid, 1989; Vol. 2, Chapter 16.
- (15) Parr, W. J. E.; Schaefer, T. *Acc. Chem. Res.* **1980**, 13, 400.
- (16) Dewar, M. J. S.; Dougherty, R. C. *The PMO Theory of Organic Chemistry*; Plenum: New York, 1975.
- (17) Dewar, M. J. S. *J. Am. Chem. Soc.* **1984**, 106, 669.
- (18) Reed, E.; Curtiss, L. A.; Weinhold, F. A. *Chem. Rev.* **1988**, 88, 899.
- (19) Reed, A. E.; Weinhold, F. *Isr. J. Chem.* **1991**, 31, 277.
- (20) Edison, S.; Markley, J. L.; Weinhold, F. *J. Biomol. NMR* **1994**, 4, 519.
- (21) Esteban, A. L.; Galache, M. P.; Mora, F.; Díez, E.; Casanueva, J.; San Fabián, J.; Barone, V.; Peralta, J. E.; Contreras, R. H. *J. Phys. Chem. A* **2001**, 105, 5298.
- (22) Wilkens, S. J.; Westler, W. M.; Markley, J. L.; Weinhold, F. *J. Am. Chem. Soc.* **2001**, 123, 12026.
- (23) Peralta, J. E.; Contreras, R. H.; Snyder, J. P. *Chem. Commun.* **2000**, 2025.
- (24) See, for example: (a) Suarez, D.; Sordo, T. L.; Sordo, J. A. *J. Am. Chem. Soc.* **1996**, 118, 9850. (b) Salzner, U. *J. Org. Chem.* **1995**, 60, 986.
- (25) Barfield, M. *J. Chem. Phys.* **1964**, 41, 3825.
- (26) Diz, C.; Ruiz de Azua, M. C.; Giribet, C. G.; Contreras, R. H. *Int. J. Quantum Chem.* **1990**, 27, 663.
- (27) Frisch, M. J.; Trucks, G. W.; Schlegel, H. B.; Scuseria, G. E.; Robb, M. A.; Cheeseman, J. R.; Zakrzewski, V. G.; Montgomery, J. A.; Stratmann, R. E.; Burant, J. C.; Dapprich, S.; Millam, J. M.; Daniels, A. D.; Kudin, K. N.; Strain, M. C.; Farkas, O.; Tomasi, J.; Barone, V.; Cossi, M.; Cammi, R.; Mennucci, B.; Pomelli, C.; Adamo, C.; Clifford, S.; Ochterski, J.; Petersson, G. A.; Ayala, P. Y.; Cui, Q.; Morokuma, K.; Malick, D. K.; Rabuck, A. D.; Raghavachari, K.; Foresman, J. B.; Cioslowski, J.; Ortiz, J. V.; Stefanov, B. B.; Liu, G.; Liashenko, A.; Piskorz, P.; Komaromi, I.; Gomperts, R.; Martin, R. L.; Fox, D. J.; Keith, T.; Al-Laham, M. A.; Peng, C. Y.; Nanayakkara, A.; Gonzalez, C.; Challacombe, M.; Gill, P. M. W.; Johnson, B. G.; Chen, W.; Wong, M. W.; Andres, J. L.; Head-Gordon, M.; Replogle, E. S.; Pople, J. A. *Gaussian 98*, Revision A.7; Gaussian, Inc.: Pittsburgh, PA, 1998.
- (28) (a) Lazzaretti, P.; Zanasi, R. *J. Chem. Phys.* **1982**, 77, 2448. (b) Lazzaretti, P. *Int. J. Quantum Chem.* **1979**, 15, 181. (c) Lazzaretti, P. *J. Chem. Phys.* **1979**, 71, 2514.
- (29) Contreras, R. H.; Peralta, J. E. *Prog. NMR Spectrosc.* **2000**, 37, 321.
- (30) Glendening, E. D.; Reed, A. E.; Carpenter, J. E.; Weinhold, F. *NBO*, version 3.1.
- (31) Jörgensen, P.; Simons, J. *Second Quantization Based Methods in Quantum Chemistry*; Academic Press: New York, 1981; Chapter 6.
- (32) Sproviero, E. M.; Ferrara, A.; Contreras, R. H.; Burton, G. *J. Chem. Soc., Perkin Trans. 2* **1996**, 933, and references therein.
- (33) (a) Karplus, M. *J. Chem. Phys.* **1960**, 33, 1842. (b) Karplus, M. *J. Chem. Phys.* **1969**, 50, 3133.
- (34) Barfield, M.; Dean, A. M.; Fallick, C. J.; Spear, R. J.; Sternhell, S.; Westerman, P. W. *J. Am. Chem. Soc.* **1975**, 97, 1482.